Journal of Hydroscience and Hydraulic Engineering
Vol. 17, No.1 May, 1999, 73-85

ESTIMATION OF A DEBRIS FLOW HYDROGRAPH AND ANALYSIS OF EVACUATION ACTION USING GIS

By

Hajime Nakagawa, Tamotsu Takahashi, Toyoaki Sawada

Disaster Prevention Research Institute, Kyoto University, Gokasho, Uji City, Kyoto, Japan

and

Akichika Ishibashi

Nippon Koei Co., Ltd., Research and Development Center, Takasaki 2304, Kukisaki Town, Ibaragi, Japan

SYNOPSIS

To compute the hazard area, a numerical simulation model that estimates a debris flow hydrograph by assigning an arbitrary rainfall to an arbitrary, very steep basin was developed. The debris flow hydrograph is not much affected by the scale of a surface landslide but is strongly affected by the position and number of landslides. Moreover, a numerical simulation model that estimate a hazard area by using the hydrograph as an input boundary condition. When applied to an actual event, this model reproduced the actual deposition situation in the fan area reasonably well. Non-structural countermeasures, such as residents of the hazard area taking refuge before debris flow flooding, are effective for saving lives. A simulation method for evacuation based on a refuge network built using the GIS (Geographic Information Systems, ARC/INFO) is presented. Information on calculated evacuation results such as traveling time from the start of evacuation to arrival at a refuge, degree of congestion of a refuge route, number of refugees in each designated refuge, and etc. is very important, and the graphic tools of the GIS can provide it intelligibly for both administrators and residents.

INTRODUCTION

A serious debris flow disaster occurred along the Gamaharazawa River, a tributary of the Hime River, in Nagano Prefecture on Dec. 6, 1996. Fourteen persons working on repairs were killed, and 9 injured by this flow. It is very rare for a debris flow to occur in winter, and it is thought that the thawing of snow combined with rainfall was one cause of this debris flow (1, 2). On May 11, 1997, a debris flow was induced by a massive landslide along the Kumazawa River, Kaduno City, Akita Prefecture. In spite of its large scale (2,500,000 m^3) and that of the subsequent debris flow (500,000 m^3 in sediment volume) that destroyed 16 houses, no deaths or injuries were reported because the landslide had been observed, and residents had already evacuated their homes (3).

Another severe debris flow disaster occurred on the Harihara River, Izumi City, Kagoshima Prefecture at midnight July 10, 1997. Twenty-one persons were killed, and 18 houses destroyed by this flow which, due to heavy rainfall, was caused by a massive slope failure with a sediment volume of 160,000 m^3. Residents were aware of an extraordinary phenomenon occurring in the river and took refuge, but they returned home because it stopped raining and water depth of the river became normal level resulting in much material and human damage (4).

In order to mitigate the flood hazards generated by debris flows, erosion control works must be undertaken as well as river improvement works. In fact, such structural countermeasures have mitigated, even prevented, disasters. Financial concerns and social situations do not always allow prompt implementation of structural mitigation measures, therefore hazard avoidance, including regulation and zoning restriction of development in the potential hazard zone, and an evacuation program are required. These 'soft' non structural measures are only

effective when reliable information is available concerning 1) the locations of hazardous and safe areas, 2) the degree of danger, 3) the potential danger period, 4) the time needed for evacuation, 5) the potential for casualties, and 6) whether evacuation systems as well as systems for the prediction of disasters are adequate. In other words, reliable hazard map and, if possible, a risk map must first be prepared, after which the best type of evacuation system can be established for the hazard area.

We present numerical methods for simulating the occurrence of debris flows, and spatial and temporal effects of a landslide on the debris flow hydrograph generated are examined. Moreover, prediction method of a debris flow flooding area on the Tochio debris fan, Gifu Prefecture, is presented. A simulated evacuation method based on a GIS network consisted of refuges, evacuation routes, and nodes in the hazard area also is presented.

BASIC EQUATIONS

Because a debris flow is considered to move as a continuous fluid until just before it stops, a system of momentum and mass conservation equations for fluid flow which take into account the variation in discharge as well as the quality of the fluid owing to erosion and deposition is applicable. The basic equations used to calculate the development and deposition of a debris flow and its flooding are depth-averaged two-dimensional momentum and continuity equations:

$$\frac{\partial M}{\partial t}+\beta\frac{\partial(uM)}{\partial x}+\beta\frac{\partial(vM)}{\partial y}=gh\sin\theta_{bx0}-gh\cos\theta_{bx0}\frac{\partial(z_b+h)}{\partial x}-\frac{\tau_{bx}}{\rho_T} \tag{1}$$

$$\frac{\partial N}{\partial t}+\beta\frac{\partial(uN)}{\partial x}+\beta\frac{\partial(vN)}{\partial y}=gh\sin\theta_{by0}-gh\cos\theta_{by0}\frac{\partial(z_b+h)}{\partial y}-\frac{\tau_{by}}{\rho_T} \tag{2}$$

$$\frac{\partial h}{\partial t}+\frac{\partial M}{\partial x}+\frac{\partial N}{\partial y}=i\{C_*+(1-C_*)S_b\}+r \tag{3}$$

The continuity of the coarse particle fraction sustained in the flow by the action of particle encounters is

$$\frac{\partial(C_Lh)}{\partial t}+\frac{\partial(C_LM)}{\partial x}+\frac{\partial(C_LN)}{\partial y}=\begin{cases} iC_{*L} & (i\geq 0)\\ iC_{*DL} & (i<0)\end{cases} \tag{4}$$

The continuity of the fine particle fraction sustained in the flow by turbulence is

$$\frac{\partial\{(1-C_L)C_Fh\}}{\partial t}+\frac{\partial\{(1-C_L)C_FM\}}{\partial x}+\frac{\partial\{(1-C_L)C_FN\}}{\partial y}=\begin{cases} i(1-C_{*L})C_{*F} & (i\geq 0)\\ i(1-C_{*DL})C_F & (i<0)\end{cases} \tag{5}$$

where $M=uh$ and $N=vh$ are the x and y components of the flow flux; u and v = the x and y components of mean velocity; h = the flow depth; z_b = the erosion or deposition thickness measured from the original bed elevation; θ_{bx0} and θ_{by0} = the x and y components of the inclination of the original bed surface; ρ_T = the density of the debris flow; β = the momentum correction coefficient; τ_{bx} and τ_{by} = the x and y components of the resistance to flow; i = the erosion (≥ 0) or deposition (<0) velocity; C_* = the volume concentration of the solids in the bed; S_b = the degree of saturation in the bed (applicable only for erosion, when deposition takes place substitute $S_b=1$); r = the water supply intensity from the side per unit length of channel (unidirectional flow case); C_L = the volume concentration of the coarse particles in the flow; C_F = the volume concentration of the fine particles in the interstitial fluid; C_{*L} and C_{*F} = the volume concentrations of the coarse and fine particles in the original bed; and C_{*DL} = the volume concentration of the coarse particles in the bed produced by the deposition of the debris flow.

Because a debris flow develops in a narrow upstream channel, its flow is virtually unidirectional (no y component), and N and v necessarily are zero. In this case the quasi-steady approximation of the equation of motion is applicable rather than equations (1) and (2) (5). The approximation for a fully developed stony debris flow is

$$u = \frac{2}{5d_L}\left[\frac{g\sin\theta}{a\sin\alpha}\left\{C_L + (1-C_L)\frac{\rho_m}{\sigma}\right\}\right]^{1/2}\left\{\left(\frac{C_{*DL}}{C_L}\right)^{1/3} - 1\right\}h^{3/2} \qquad (6)$$

and for an immature debris flow and a turbulent flow the respective approximations are

$$u = \frac{0.7\sqrt{g}}{d_L}h^{3/2}\sin^{1/2}\theta \qquad (7) \qquad u = \frac{1}{n_m}h^{2/3}\sin^{1/2}\theta \qquad (8)$$

where d_L = the mean diameter of the coarse sediment; σ = the density of the coarse particle; ρ_m = the density of the interstitial fluid including the fine particles; n_m = the resistance coefficient; a = the numerical coefficient (0.04); α = the dynamic internal angle of friction ($\tan\alpha$=0.6), and θ = the energy gradient given by $\tan\theta = \sqrt{\tau_{bx}^2 + \tau_{by}^2}/\rho_T gh$. An immature debris flow whose sediment concentration C_L is less than $0.4C_{*L}$ and greater than 0.02 occurs when 0.03¡$\tan\theta$¡0.138. Equation (8), which is nothing but the Manning formula, is applicable when C_L is less than 2% or h/d_L is larger than 30 and the flow occurs $\tan\theta$ is less than 0.03. The momentum correction coefficient, β, is equal to 1.25 for a stony type debris flow (6) and to 1.0 for both an immature debris flow and a turbulent flow.

The bottom resistance for a two-dimensional flow is described as follows. For a fully developed stony debris flow (7);

$$\tau_{bx} = \frac{\rho_T}{8}\left(\frac{d_L}{h}\right)^2 \frac{u\sqrt{u^2+v^2}}{\{C_L + (1-C_L)\rho_m/\sigma\}\{(C_{*DL}/C_L)^{1/3}-1\}^2} \qquad (9)$$

$$\tau_{by} = \frac{\rho_T}{8}\left(\frac{d_L}{h}\right)^2 \frac{v\sqrt{u^2+v^2}}{\{C_L + (1-C_L)\rho_m/\sigma\}\{(C_{*DL}/C_L)^{1/3}-1\}^2} \qquad (10)$$

For an immature debris flow;

$$\tau_{bx} = \frac{\rho_T}{0.49}\left(\frac{d_L}{h}\right)^2 u\sqrt{u^2+v^2} \qquad (11) \qquad \tau_{by} = \frac{\rho_T}{0.49}\left(\frac{d_L}{h}\right)^2 v\sqrt{u^2+v^2} \qquad (12)$$

The equation of erosion for an unsaturated bed is

$$\frac{i}{\sqrt{gh}} = K\sin^{3/2}\theta\left\{1 - \frac{\sigma-\rho_m}{\rho_m}C_L\left(\frac{\tan\phi}{\tan\theta} - 1\right)\right\}^{1/2}\left(\frac{\tan\phi}{\tan\theta} - 1\right)(C_{T\infty} - C_L)\frac{h}{d_L} \qquad (13)$$

and for a saturated one (5),

$$i = \delta_e\frac{C_{T\infty}}{C_* - C_{T\infty}}\left\{1 - \frac{C_L}{C_{L\infty}}\frac{\rho_m}{\rho}\frac{\tan\phi - (C_T/C_{T\infty})(C_{L\infty}/C_L)(\rho/\rho_m)\tan\theta}{\tan\phi - \tan\theta}\right\}\frac{q_T}{d_L} \qquad (14)$$

where K and δ_e = constants, ϕ = the angle of internal friction of sediment particle on the bed, C_T = the volume concentration of the total solids, q_T = the flow discharge per unit width, and ρ = the density of the clear water;

$$C_{T\infty} = \frac{\rho\tan\theta}{(\sigma-\rho)(\tan\phi - \tan\theta)} \qquad (15) \qquad C_{L\infty} = \frac{\rho_m\tan\theta}{(\sigma-\rho_m)(\tan\phi - \tan\theta)} \qquad (16)$$

For an immature debris flow and for a bed load, the respective equilibrium solid concentrations are

$$C_{S\infty} = 6.7C_{T\infty}^2 \qquad (17) \qquad C_{B\infty} = q_{B\infty}/(hu) \qquad (18)$$

where $q_{B\infty}$ = the equilibrium bed load transport rate. In this study the equation used is (8)

$$\frac{q_{B\infty}}{\{(\sigma/\rho-1)gd_L^3\}^{1/2}} = \frac{1+5\tan\theta}{\cos\theta}\sqrt{\frac{8}{f}}\left(1-\gamma^2\frac{\tau_{*c}}{\tau_*}\right)\left(1-\gamma\sqrt{\frac{\tau_{*c}}{\tau_*}}\right) \qquad (19)$$

where f = the resistance coefficient; τ_* and τ_{*c} = the nondimensional tractive and nondimensional critical tractive forces, and γ = a constant. Equation(17) is applicable only when $C_{S\infty}$ has a value less than $C_{T\infty}$, as calculated by eq.(15) (9).

We introduce the following deposition equations (9). For a fully developed debris flow;

$$i = \delta_d\left(1 - \frac{\sqrt{u^2+v^2}}{pv_e}\right)\frac{C_{L\infty} - C_L}{C_{*DL}}\sqrt{u^2+v^2} \qquad (20)$$

and for an immature debris flow and a turbulent flow;

$$i = \delta'_d \frac{C_{S\infty} - C_L}{C_{*DL}} \sqrt{u^2 + v^2} \qquad (21) \qquad i = \delta''_d \frac{C_{B\infty} - C_L}{C_{*DL}} \sqrt{u^2 + v^2} \qquad (22)$$

where δ'_d, δ''_d and p = constants; and v_e = the equilibrium velocity that continues the run down with neither deposition nor erosion. This is given by eq.(6) by substituting θ_e for θ, $\tan\theta_e$ being from eq.(16);

$$\tan\theta_e = \{C_L(\sigma - \rho_m)\tan\phi\}/\{C_L(\sigma - \rho_m) + \rho_m\} \qquad (23)$$

Equation for the variation of the bed surface elevation is given by $\partial z_b/\partial t + i = 0$.

AREA STUDIED

The Horadani basin (**Fig.1**) in the Northern Japan Alps has an area of 2.3 km^2 and 4 typical tributaries. The 2,675 m main channel shown in Fig.1 as ② originates at the altitude of 2,185 m and debouches at 800 m. At the outlet of the ravine a relatively large debris fan, 500 m wide, has developed that has a 9.5° average slope for the downstream direction. The community of Tochio is located on this debris fan.

On August 22, 1979 at about 7:50 in the morning at the time of peak rainfall intensity, a debris flow suddenly struck Tochio. It killed three persons, as well as destroying 7 houses, half destroying 36, and inundating 19. Spatial sediment deposition and the damage to houses are shown in **Fig.2**. The total volume of the sediment deposit was about 66,000 m^3, and the sediment volume of the landslide in the uppermost upstream part (shown in **Fig.1** as ①) which enlarged the scale of the debris flow was estimated to be about 8,740 m^3 (10), but it is not clear whether all of the sediment flowed out or not.

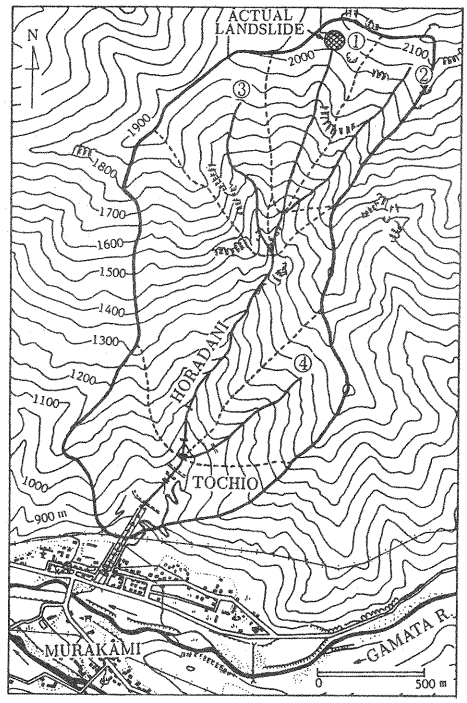

Fig.1 Area studied

DEBRIS FLOW HYDROGRAPH

Conditions for Calculations

Fig.3 shows the estimated flood runoff discharge at the outlet of the ravine based on the existing flood runoff analysis for the condition in which no debris flow has occurred. To calculate the development of the debris flow along the channel's course, a discharge hydrograph for water only is needed at each point on the course. To meet this requirement the time lag is neglected, the outlet water discharge, Q_0, is firstly assigned proportionally to the sub-basin areas of the tributaries. Next the lateral inflow discharge of water per unit width along each channel is assigned as shown in **Fig.4**, in which a main course is taken along the channel ① and landslide occurs at ①.

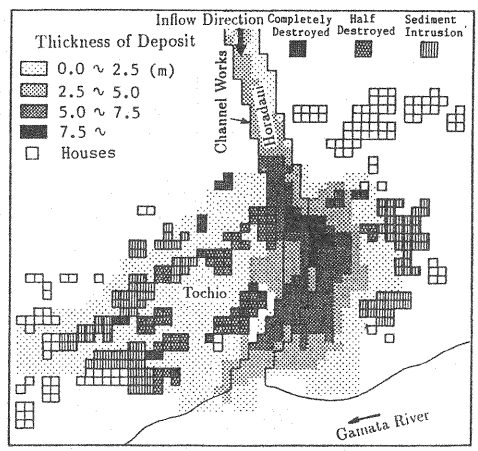

Fig.2 Thickness of the accumulated sediment and its hazard to houses

As the time at which the landslide occurred at the upstream end is not known, we assume that it took place at 7:50, at which time a debris flow of 10-second duration was introduced into the upstream end of the channel ①. A constant debris flow discharge of 400m^3/sec was assumed with $C_L = 0.5$ and $C_F = 0$. The channel characteristics of flow width, and thickness, and the properties of the sediment are estimated from field and aerial photograph surveys. A uniform channel width of 10 m is assumed from the upstream to downstream end, and the bed sediment

is assumed to be 4m thick with the properties $d_L = 10$cm, $C_* = 0.65$, $C_{*DL} = 0.65$, $C_{*F} = 0.2$, $C_{*L} = (C_* - C_{*F})/(1 - C_{*F}) = 0.5625$, $\tan\phi = 0.75$, $\sigma = 2.65\mathrm{g/cm^3}$, $\rho = 1.0\mathrm{g/cm^3}$ for all the tributaries. The degree of saturation is assumed to be $S_b = 1.0$ for a bed with a slope flatter than 21° and 0.8 for a steeper bed.

The values of K in eq.(13) and δ_e in eq.(14) were identified in previous flume experiments as $K = 0.05$ and δ_e =0.0007 (5). A sensitivity analysis determined that these values could be applied to debris flows; therefore, they were used in the analysis of the effects of the landslide on the debris flow hydrograph. A one dimensional finite difference calculation for the river channel was made with grids of $\Delta x = 50$ m and $\Delta t = 0.2$ sec. In this calculation the numerical constant values adopted were $\delta_d' = \delta_d'' = 0.1$ and $p = 1/3$ (9).

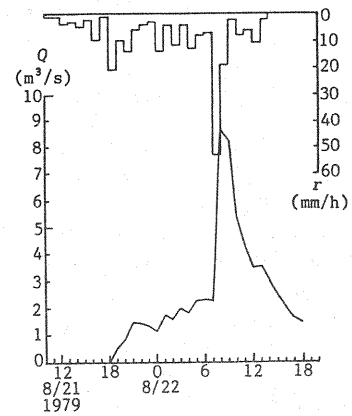

Fig.3 Calculated flood hydrograph at the top of the fan

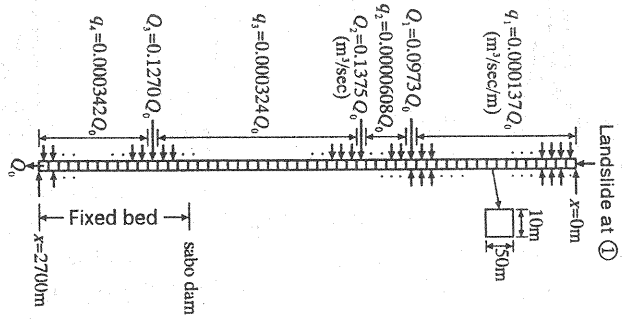

Fig.4 Flood discharge variation along the main stream channel

Effects of Landslide Scale on the Debris Flow Hydrograph

Fig.5 shows effects of the sediment volume of the landslide, which corresponds to the landslide scale, on the debris flow hydrograph at the outlet of the ravine. The position of the landslide and the method of supplying landslide sediment to the upstream end of the channel in the calculation are the same as described previously, but the sediment volume supplied is different. A supplying sediment volume range of 1,000 ~ 4,000 m³ (substantial sediment volume) for a surface landslide caused by a heavy rainfall is considered to cover the possible scale of the supplied sediment volume. From this figure, the sediment volume of the landslide, therefore, does not have a marked effect on the debris flow hydrograph

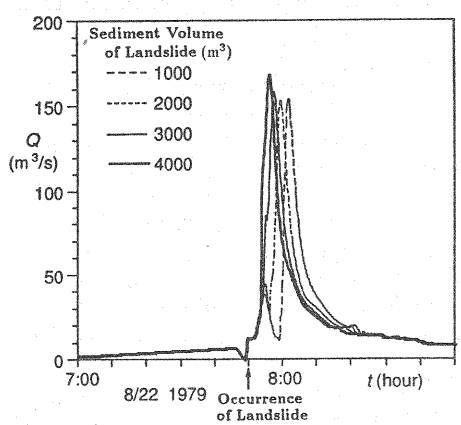

Fig.5 Effect of landslide sediment volume on the debris flow hydrograph

Effects of Landslide Position on the Debris Flow Hydrograph

Fig.6 shows effects of the landslide location in the watershed on the debris flow hydrograph at the outlet of the ravine. The position of the sediment supply given by ①~④ in Fig.1 is the upstream end of each channel. Because a debris flow hydrograph generated by erosion of the bed material depends on the sediment volume on the bed and the water discharge in the channel, the debris flow hydrograph produced by the landslide at ④ has a smallest peak discharge, in which the channel length is the shortest. On the other hand, the debris flow generated by the landslide at ② has the highest peak discharge because it has the longest channel length, namely,

that has the largest erodible sediment volume on the bed if the water discharge in the channel is enough to generate a debris flow.

Effects of the Number of Landslides on the Debris Flow Hydrograph

Fig.7 shows debris flow hydrographs calculated for conditions under which two landslides occur at ① and ②. One case is for two landslides that occur at the same time, the other is for a landslide at ② that occurs 10 minutes later than that at ①. The peak discharge of the debris flow is higher in the former case. In the latter, the hydrograph has two peaks, a first peak due to the landslide at ① and a second due to the landslide at ②.

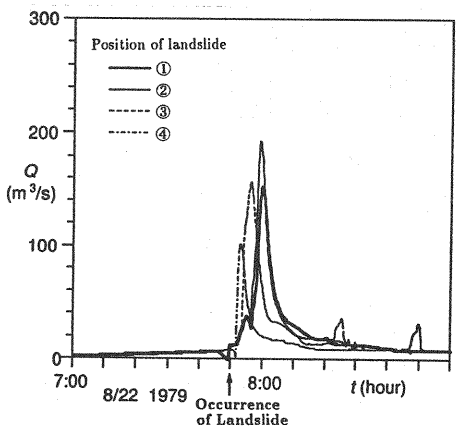

Fig.6 Effect of landslide position on the debris flow hydrograph

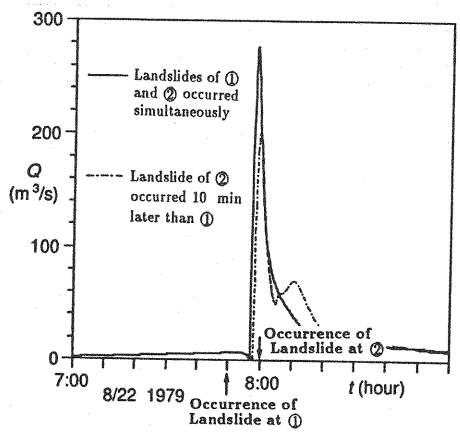

Fig.7 Effect of the time of occurrence and number of landslides on the debris flow hydrograph

PREDICTION OF FLOODING IN A HAZARD AREA

Neither how many surface landslides may occur nor when or where are identified in this study. We examined two types of landslides; one in which a surface landslide occurs at ① (CASE-1), corresponding to the actual event of 1979, and one in which landslides occur simultaneously at ① and ② (CASE-2).

The calculated hydrograph and solids concentrations in the debris flow at the outlet of the ravine constitute the upstream boundary conditions for flooding calculations on the debris fan at Tochio. The flooding process and deposition on the fan were computed using a two-dimensional numerical simulation, and a staggered up-wind finite difference scheme (9). The grid sizes are $\Delta x = \Delta y = 5\,\mathrm{m}$, $\Delta t = 0.02$ sec.

Fig.8 shows the calculated results of final stage of the sediment deposition by the debris flow flooding for CASE-1. A comparison with **Fig.2** shows that both the area of inundation and deposit depths are reasonably well reproduced by the calculations.

Fig.9 shows the calculated results of final stage of the sediment deposition by the debris flow flooding for CASE-2. The peak discharge of the debris flow hydrograph used in this calculation is about twice that in CASE-1. The total sediment volume outflow is about 70,000m^3 in CASE-2 and about 50,000m^3 in CASE-1. The deposit thickness is greater in CASE-2, but the depositional area does not differ substantially from that in CASE-1. We conclude that the representative features of the depositional area and the thickness of deposits produced by a typical debris flow in this basin are well approximated by this figure.

SIMULATION OF EVACUATION USING THE GIS

Refuge Network Based on the GIS

In our research on a simulation method for evacuation action during overland flood flows and mud flows (12, 13), the refuge networks were established by man-power. Very careful treatment and much labor were needed to check the relationship between the node and arc numbers. In contrast, refuge networks can very easily be established with the aid of a GIS, in which the

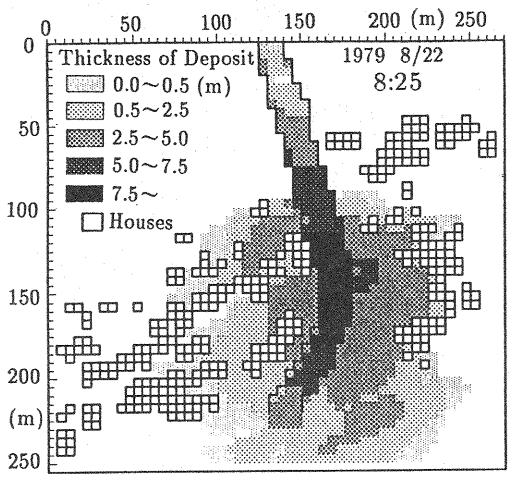

Fig.8 Calculated sediment accumulation in CASE-1

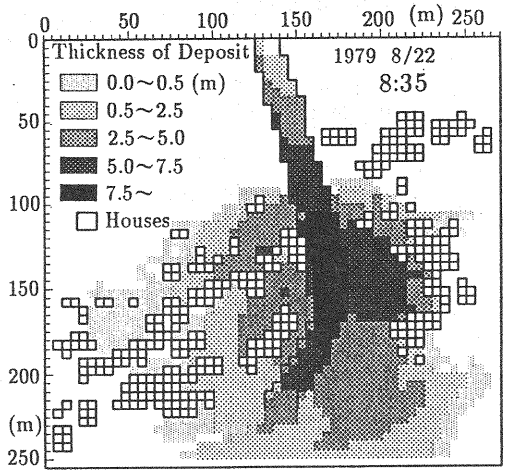

Fig.9 Calculated sediment accumulation in CASE-2

relationship is checked automatically when nodes are input by a digitizer. This method saves much time and trouble in managing and updating complicated data.

Fig.10 shows an example of a refuge network comprised of nodes of the intersection point and vertexes, and those of the places of refuge. By inputting the data on nodes and vertexes using the digitizer, tables (arc attribute, node attribute tables, etc.) can be made in which node numbers are automatically set in correspondence to arc numbers. The most important point is that not only are refuge networks very easily established by the GIS and networks made available for evacuation calculations because the coordinates of the nodes and arcs are stored as ASCII data, but the calculated results of evacuation action can be displayed on the GIS's coverage.

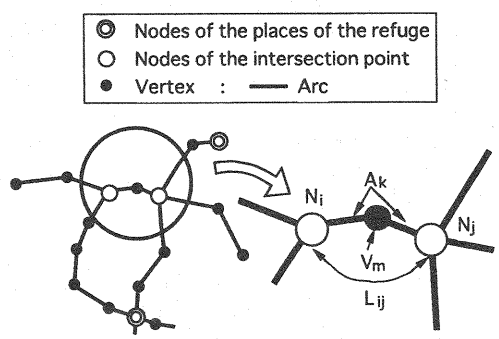

Fig.10 Example of the nodes, vertexes, and arcs in the refuge network

Simulation Method of the Action of Evacuation

Refuge networks constructed with the aid of a GIS consisted of refuges, evacuation routes, and nodes in the hazard area. The hazard evacuation area was determined by the numerical simulation of sediment flooding. Refuges (e.g., schools, public offices) had been designated in the existing Regional Plan for Disaster Prevention.

Adequacies of the refuges and evacuation routes are evaluated in relation to the calculated flow depth, deposit thickness, and evacuation simulation. For example, buried refuges or evacuation routes would be unsuitable, and new refuges or routes would have to be established. This simulation model therefore provides a reasonable foundation on which to plan better evacuation systems.

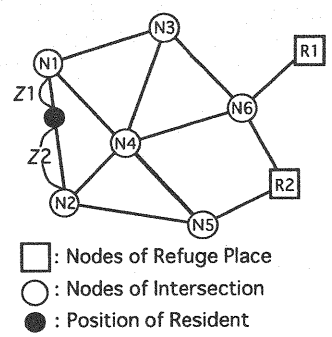

Fig.11 Relationship between the refuge network and the position of an evacuee

The distance between the locations of the residents and the refuges generally is one of the most important factors for selecting a particular refuge. It is assumed that the method of selection of optimal refuge can be formulated as a selection problem of shortest-path algorithms in network theories. **Fig.11** shows an example of the position of a group of residents *en route* on the refuge network. The group is located at the distance $Z1$ from the node of **N1** and at the distance $Z2$ from the node of **N2**. The simulated evacuation action is

(a) The shortest distance from an arbitrary position between nodes **N1** and **N2** to an arbitrary

refuge node is calculated by

$$FF = \min\{F_{N1,1} + Z1, \cdots, F_{N1,m} + Z1, F_{N2,1} + Z2, \cdots, F_{N2,m} + Z2\} \qquad (24)$$

where FF = the shortest distance from an arbitrary position between the node of **N1** and **N2** on the refuge route to an arbitrary refuge node; $F_{i,j}$ = the shortest distance between an intersection node, **Ni**, and a refuge node, **Nj**, as found by the Warshall-Floyd method (13) and m = the total number of refuges.

(**b**) Assuming that the solution of eq.(24) is $F_{N1,R1} + Z1$ (i.e., the shortest path is the approach route to refuge node **R1** through intersection node **N1**). Time TL required to move from the position of the group to node **N1** is calculated from the walking speed of the evacuating group, the details of which are described later.

(**c**) Let T be the time set to calculate the evacuating action: if $TL > T$ (i.e., an evacuating group can not arrive at node **N1** within time T) a new position between the last position and **N1** is calculated from the value T and the walking speed. But, if $TL < T$, the evacuating group can reach node **N1**, and time remains which can be used for further motion. If **N1** is a refuge, the evacuating action of this group is finished; if not, $T - TL$ is replaced by a new T and going back to (**a**), the remaining time is consumed in proceeding through **N1**.

This procedure is repeated making it possible to simulate the evacuation action of residents.

Walking Speed

Walking speed during evacuation is affected by various types of factors: environmental ones such as the season, weather, time, brightness; physical factors such as sex, age, health, fatigue; collateral factors such as clothes, baggage; psychological factors such as fear, whether the place is well known; and factors of assembly such as the number of persons in the group, and the density of people on the road. It is very difficult to correctly estimate walking speed in the midst of evacuation because these affecting factors are interconnected.

In this calculation, the walking speeds of an adult, a child, and an elderly person are introduced in the cases of solitary walking and group one. Moreover, a reduction rate of walking speed due to congestion on the evacuation route and fatigue are considered. **Fig.12** shows the walking speeds of elderly persons in solitary walking and group walking (14). The curves in this figure are calculated results of frequency of walking speeds assuming a normal distribution and using the observed values of the parameters of the mean walking speed, $\overline{U}_0$, and the variance, σ_u^2. The mean walking speed of an elderly person in the case of solitary walking is 0.948 m/sec and the variance 0.045 $(\mathrm{m/sec})^2$, whereas the values in the case of group walking are 0.751 m/sec and 0.021 $(\mathrm{m/sec})^2$. Walking speed in the group walking case is slower than it is for solitary walking, and the variance becomes smaller. **Fig.13** shows walking speeds of persons with a baby carriage or a child (14). The mean walking speed of a person with children is 1.02 m/sec and the variance is 0.036 $(\mathrm{m/sec})^2$. The density of the persons evacuating on the refuge route is said to affect the walking speed markedly.

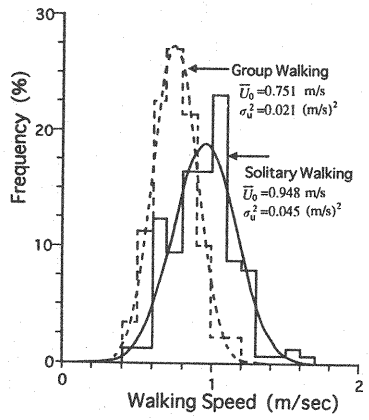

Fig.12 Frequency of the walking speeds of elderly persons in cases of solitary and group walking

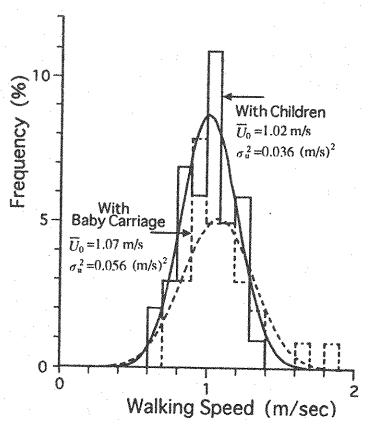

Fig.13 Frequency of the walking speeds of persons with a baby carriage or with a child

In this study the walking speed is defined as (15)

$$V_n^t = U_n^t/\{0.982 + \exp(1.12t - 4.0)\} \quad (\text{unit:}t;\text{hour}, V_n^t, U_n^t;\text{m/s}) \tag{25}$$

$$U_n^t = \begin{cases} \overline{U}_0 - C\rho_n^t & (\rho_n^t < \rho_{\max}) \\ \overline{U}_{\min} & (\rho_n^t \geq \rho_{\max}) \end{cases} \tag{26}$$

where V_n^t = the walking speed of a group on the nth route at time t; t = the time elapsed since evacuation began; U_n^t = the walking speed of a group on the nth route at time t, which depends on the density of people on the route but is independent of fatigue; and $\overline{U}_0$ = the initial walking speed of 1.42 m/sec for an adult, 0.948 m/sec for an elderly person walking alone, 0.751 for an elderly person walking in a group and 1.02 m/sec for a person with children. Walking speed depends on the minimum value when elderly persons or children are included in the group. $\overline{U}_{\min}$ = the minimum walking speed of the group, assuming the value of 0.49 m/sec; ρ_n^t = the density of people in the group on the nth route at time t, written $\rho_n^t = M_n^t/(B_n L_n)$, (unit: person/m^2), in which M_n^t = the total number of evacuees on the nth route at time t; B_n = the width of the nth route (unit:m); L_n = the length of the nth route (unit:m); C = the coefficient describing the reduction rate of walking speed due to congestion, written $C = (\overline{U}_0 - \overline{U}_{\min})/\rho_{\max}$; and $\rho_{\max}$ = the allowable maximum density of people, assuming the value of 3.85 person/m^2.

Conditions for Calculations

Fig.14 shows a map of the Tochio district and its outskirts. This district has 79 households and a population of 272. Thirty-seven percent of the population consists of children and the elderly. The respective values for the Kashiwade and Murakami districts are 17 and 25 for households, and 42 and 118 for population. The number of households and the organization of persons in each district are shown in **Table 1.**

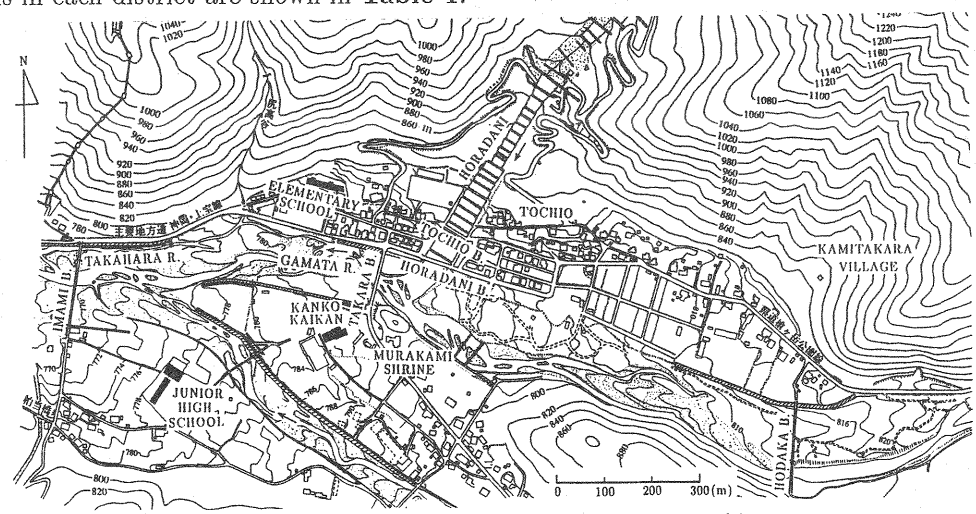

Fig.14 Map of the Tochio district and its outskirts

Fig.15 gives an example of the refuge network in the Tochio district and its outskirts. The number of intersection nodes totals 490. Three of them, Tochio elementary school, Tochio junior high school, and Kanko Kaikan are the refuges designated in the Regional Plan for Disaster Prevention of the municipal government. The minimum unit of residents is here defined as a family (one household), therefore the number of refuge group is 121.

Table 1 Number of households and the persons in each district

District		Tochio	Murakami	Kashiwade	Total
Number of Household		79	25	17	121
Constitution	Adult	171	61	25	257
	Child	49	22	6	77
	Elderly	52	35	11	98
	Total	272	118	42	432

The simulation cases are shown in **Table 2.** CASEs 1, 2, 5, and 6 denote that residents choose the nearest place of refuge, and CASEs 3 and 4 that residents can not choose Tochio junior high school or Kanko Kaikan due to river flooding and must select Tochio elementary school as the

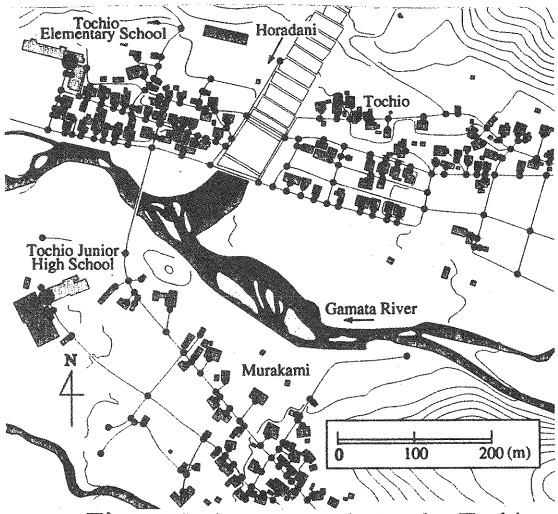

Fig.15 Refuge networks in the Tochio district and its outskirts

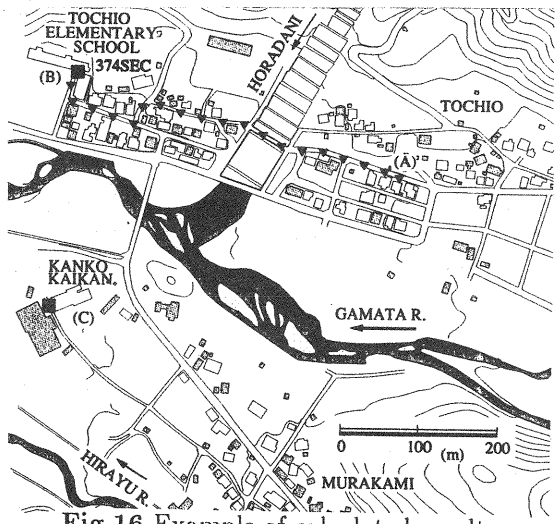

Fig.16 Example of calculated results of the state of evacuation

place of refuge. CASEs 1, 3, and 5 are those in which the initial walking speed of all the residents is assumed to be 1.42 m/sec (walking speed of an adult). CASEs 2,4, and 6 are those in which the initial walking speeds of elderly persons or children are considered. CASEs 5 and 6 are those in which a new refuge place is established on the east side of the Horadani River in the Tochio district. In these cases, we consider that all the residents start to take refuge simultaneously.

Fig.16 shows the position of a resident who has evacuated his/her home (A) and that of refuge (B) (Tochio elementary school) at 20 second intervals (position: ▼, refuge: ■). In this case it takes 374 seconds to arrive at the refuge. The calculated results are shown in **Table 2**. All the residents in the Tochio district move to this refuge (B) because it is the closest one. The maximum traveling time from the start of evacuation to arrival is 1,588 seconds in CASEs 2 and 4. This traveling time increases more than 1.5-fold when the walking speeds of elderly persons or children are considered. Residents of the Murakami district move to refuge (C) (Kanko Kaikan) in the case in which they can select the nearest refuge. The maximum traveling time is 805 seconds to this refuge, whereas it takes 1,216 seconds when they have to evacuate to Tochio elementary school.

Table 2 Conditions for calculations and the calculated results

CASE No.	Condition of Evacuation	District	Mean Time[1] (sec)	Max Time[2] (sec)
1	Walking Speed: Adult Selection of Refuge Place: The Nearest Refuge Place	Tochio	378	839
		Murakami	292	426
		Kashiwade	277	515
		Whole	346	839
2	Walking Speed: Adult, Old People, Children Selection of Refuge Place: Same as in CASE 1	Tochio	548	1588
		Murakami	473	805
		Kashiwade	434	767
		Whole	516	1588
3	Walking Speed: Same as in CASE 1 Selection of Refuge Place: Tochio Elementary School	Tochio	378	839
		Murakami	493	644
		Kashiwade	711	837
		Whole	449	839
4	Walking Speed: Same as in CASE 2 Selection of Refuge Place: Same as in CASE 3	Tochio	548	1588
		Murakami	795	1216
		Kashiwade	1113	1585
		Whole	678	1588
5	Walking Speed: (CASE 1) Selection of Refuge Place: Same as in CASE 1 Add One More Refuge Place	Tochio	145	395
		Murakami	292	426
		Kashiwade	277	515
		Whole	193	515
6	Walking Speed: (CASE 2) Selection of Refuge Place: Same as in CASE 1 Add One More Refuge Place	Tochio	209	747
		Murakami	473	805
		Kashiwade	434	767
		Whole	295	767

Mean Time[1] : Mean Time Required for Evacuation
Max Time[2] : Maximum Time Required for Evacuation

The calculated results of the distributions of the time required for evacuation in CASEs 2 and 6, show that 15 minutes can be saved by establishing a new place of refuge in the Tochio district on the east side of the Horadani River. These results need to be verified from records of evacuation training. The graphic display based on the GIS (ARC/INFO) and EWS provides both municipal government administrators and residents an understanding of the evacuation systems in the basin.

CONCLUSIONS

A mathematical model is proposed for the prediction and assessment of debris flow hazards. Debris flow hydrographs were analyzed by assigning an arbitrary rainfall to an arbitrary, very steep basin. Spatial and temporal effects of a landslide on the debris flow hydrograph generated

were examined. The magnitude of the landslide was shown to have no significant effect on the hydrograph, whereas the location and number of landslides substantially affected the peak discharge of the hydrograph, timing of its occurrence, and the shape of the hydrograph.

A two-dimensional numerical simulation of a historical debris flow accurately replicated its fan deposits. The depositional characteristics of the historical event were analyzed with the model. The use of this model requires many parameter values and constants, the standard values of which are matters for future investigation. Moreover, we had to assume the time at which the landslide occurred as well as its sediment volume and water content in order to obtain a debris flow that matched the actual records. Predictions of the time of occurrence, magnitude, quality, and location of the landslide(s) under given rainfall and basin characteristics are difficult to verify. Our proposed method, however, is effective for obtaining a risk assessment in a river basin and for designing such appropriate countermeasures against debris flow as evacuation systems.

An evacuation model was developed using a GIS refuge network. The optimum refuge route and place, as well as the time required for evacuation can be obtained with this model. These findings should be made available to both residents and administrators. A visual evacuation display using a GIS model is a very useful for helping administrators and residents to understand or improve the actual evacuation system in the basin.

REFERENCES

1. Kawakami, H.: The Debris Flow Disaster at Otari Village, Nagano Prefecture, 1996, Research Report on Natural Disasters, Supported by the Japanese Ministry of Education, Science, Sports and Culture (Grant No.08300017), pp.1-1–13-3, 1997 (in Japanese).
2. Egashira, S.: The 1996 Gamaharazawa Debris Flow Hazard in Nagano, Jour. of JSCE, Vol.83, Feb., pp.49–54, 1998 (in Japanese).
3. Imamura, F. : Preliminary report on damage by debris flow in the Kumazawa River, Akita Prefecture, Jour. of Japan Society for Natural Disaster Science, Vol.16, No.2, pp.101–106, 1997 (in Japanese).
4. Iwamatsu, A. : 1997 debris flow disaster along the Harihara River, Izumi City, Kagoshima Prefecture, Japan, Jour. of Japan Society for Natural Disaster Science, Vol.16, No.2, pp.107–111, 1997 (in Japanese).
5. Takahashi, T., H. Nakagawa and S. Kuang : Estimation of debris flow hydrograph on a varied slope bed, Proc. of the Corvallis Symposium on Erosion and Sedimentation in the Pacific Rim, pp.167–177, 1987.
6. Takahashi, T. : The mechanism of the occurrence of mud-debris flows and their characteristics in motion, Annuals of the Disaster Prevention Research Institute, Kyoto Univ., 20B-2, pp.405–435, 1977 (in Japanese).
7. Takahashi, T. : Debris Flow, Balkema, Rotterdam, pp.1–165, 1991.
8. Takahashi, T. : High velocity flow in steep erodible channels, Proc. of 22nd Congress of IAHR, Lausanne, pp.42–53, 1987.
9. Takahashi, T., H. Nakagawa, T. Harada and Y. Yamashiki : Routing debris flows with particle segregation, Jour. of Hydraulic Engineering, ASCE, Vol.118, No.11, pp.1490–1507, 1992.
10. Jindu River Sabo Office, Ministry of Construction and Regional Development Consultants, Co.Ltd. : A report of the field investigation of the Horadani debris flow disaster on August 22, 1979, pp.1–128, 1979 (in Japanese).
11. Takahashi, T., H. Nakagawa and M. Higashiyama : Simulation of Group Evacuation Linked with an Inundation Analysis, Proc. of the Japan Conference of Hydraulics, Vol.33, pp.355–360, 1989 (in Japanese).
12. Takahashi, T., H. Nakagawa, M. Higashiyama and H. Sawa : Assessment of evacuation systems for water or mud floods: a combined simulation of flooding and the action of residents, Jour. of Natural Disaster Science, Vol.12, No.2, pp.37–62, 1990.
13. Iri, M. and T. Kobayashi : The network theory, OR library 12, Nikkagiren, pp.47–52, 1976 (in Japanese).
14. Institute for Fire Safety and Disaster Preparedness : Comprehensive bibliography of regional disaster prevention data, series on regional evacuation, pp.93–94, 1987 (in Japanese).
15. Nishihara, T. : Evacuation systems based on analyses of inundation, Doctoral thesis, Kyoto University, pp.166–177, 1983 (in Japanese).

APPENDIX–NOTATION

The following symbols are used in this paper:

a	=	numerical coefficient (=0.04);
B_n	=	width of the nth route (unit: m);
C	=	coefficient describing the reduction rate of walking speed due to congestion;
C_F	=	volume concentration of the fine particles in the interstitial fluid;
$C_{B\infty}$	=	equilibrium solid concentration of the bed load;
C_L	=	volume concentration of the coarse particles in the flow;
$C_{L\infty}$	=	equilibrium solid concentration of the stony debris flow;
$C_{S\infty}$	=	equilibrium solid concentration of the immature debris flow;
C_T	=	volume concentration of the total solids;
$C_{T\infty}$	=	equilibrium concentration of the total solids;
C_*	=	volume concentration of the solids in the bed;
C_{*F}	=	volume concentration of the fine particles in the original bed;
C_{*L}	=	volume concentration of the coarse particles in the original bed;
C_{*DL}	=	volume concentration of the coarse particles in the static bed produced by debris flow deposition;
d_L	=	mean diameter of the coarse particles;
f	=	resistance coefficient;
$F_{i,j}$	=	the shortest distance between the intersection node, **Ni**, and refuge node, **Nj**;
FF	=	the shortest distance from an arbitrary position on the refuge route to an arbitrary refuge node;
g	=	gravitational acceleration;
h	=	flow depth;
i	=	erosion (≥ 0) or deposition (< 0) velocity;
K	=	numerical constant;
L_n	=	length of the nth route (unit: m);
m	=	total number of refuges;
M, N	=	respective flow discharge per unit width in the x and y directions;
M_n^t	=	total number of residents on the nth route at time t;
n_m	=	resistance coefficient on the bed for the turbulent flow:
p	=	numerical constant;
$q_{B\infty}$	=	equilibrium bed load transport rate;
q_T	=	flow discharge per unit width;
r	=	water supply intensity from the side per unit length of channel;
S_b	=	degree of saturation in the bed;
t	=	time;
T	=	time set to calculate the evacuating action;

TL = time required to move from the position of the group to the nearest node;
u, v = respective mean velocity components in the x and y directions;
U_n^t = walking speed without fatigue of a group on the nth route at time t;
$\overline{U}_0$ = initial walking speed;
$\overline{U}_{\min}$ = minimum walking speed of a group (=0.49 m/sec);
v_e = equilibrium velocity that continues the run down with neither deposition nor erosion;
V_n^t = walking speed of a group on the nth route at time t;
x, y = coordinates of the flow;
z_b = erosion or deposition thickness measured from the original bed elevation;
$Z1, Z2$ = respective distances from the position of the group to nodes **N1** and **N2** in **Fig.10**;
α = dynamic internal angle of friction ($\tan\alpha$=0.6);
β = momentum correction coefficient;
γ = numerical constant;
δ_d = numerical constant of the equation of deposition;
δ_d' = numerical constant of the equation of deposition;
δ_d'' = numerical constant of the equation of deposition;
δ_e = numerical constant of the equation of erosion;
Δt = time interval in the finite difference equations;
$\Delta x, \Delta y$ = respective spatial mesh sizes in the x and y directions in the finite difference equations;
$\theta_{bx0}, \theta_{by0}$ = respective inclination of the original bed surface in the x and y directions;
θ = energy gradient given by $\tan\theta = \sqrt{\tau_{bx}^2 + \tau_{by}^2}/\rho_T g h$;
θ_e = equilibrium angle of the bed surface;
ρ = density of the clear water;
ρ_m = density of the interstitial fluid ($= \rho(1 - C_F) + \sigma C_F$);
$\rho_{\max}$ = allowable maximum density of people (=3.85 person/m^2);
ρ_n^t = density of people in the group on the nth route at time t;
ρ_T = density of the debris flow ($= \rho_m(1 - C_L) + \sigma C_L$);
σ = density of the coarse and fine particles;
σ_u^2 = variance in walking speed;
τ_{bx}, τ_{by} = respective shear stresses on the bed surface in the x and y directions;
$\tau*$ = nondimensional tractive force;
$\tau*c$ = nondimensional critical tractive force; and
ϕ = angle of internal friction of sediment particles on the bed.

(Received October 19, 1998 ; revised January 11, 1999)